ON A COMPARISON OF NUMERICAL SIMULATIONS OF ATMOSPHERIC FLOW OVER COMPLEX TERRAIN

T. Bodnár, L. Beneš and K. Kozel
Department of Technical Mathematics, Faculty of Mechanical Engineering,
Czech Technical University in Prague

Introduction

This paper presents an introduction to a comparative study of numerical codes designed to solve the Atmospheric Boundary Layer (ABL) flow in a proximity of complex terrain. The main aim is to check what are the major differences between the predictions of different mathematical models and what is the effect of various discretization methods on numerical results. This is a basic step towards a detailed comparison of numerical simulations with either experimental results obtained either on scaled down wind-tunnel model, or real size scaled data obtained during on-location measurements.

Mathematical model(s)

The mathematical model for all of the numerical solvers presented here is based on the Reynolds Averaged Navier-Stokes (RANS) equations. The turbulent closure differs from code to code. The following governing system describes the flow of turbulent, incompressible media. It consists of the conservation mass and linear momentum written using Reynolds-Averaged mean quantities, i.e. velocity $\boldsymbol{v} = col(u, v, w)$ and pressure p. The density ρ is considered constant in this case. The volume forces (gravity, Coriolis, etc.) are neglected.

The resulting system can be written in conservative form as:

$$\boldsymbol{\nabla} \cdot \boldsymbol{v} = 0 \tag{1}$$

$$\frac{\partial \rho \boldsymbol{v}}{\partial t} + \boldsymbol{\nabla} \cdot (\rho \boldsymbol{v} \otimes \boldsymbol{v}) = -\boldsymbol{\nabla} p + \boldsymbol{\nabla} \cdot \left[K \left(\boldsymbol{\nabla} \boldsymbol{v} + \boldsymbol{\nabla}^T \boldsymbol{v} \right) \right] \tag{2}$$

The turbulent diffusion $K = \mu + \mu_T$ is equal to sum of molecular (laminar) viscosity μ and turbulent (eddy) viscosity μ_T. The turbulent viscosity is evaluated using suitable turbulence model.

Algebraic mixing length turbulence model

This model was chosen because of its simplicity and adaptation to atmospheric flows including stratification.

According to idea of Prandtl[1] we assume here the fluid parcel is an entity that moves a distance (*mixing length*) ℓ keeping its original momentum. So the mixing length is in some way

[1] See e.g. the classical book [6]

analogous to the mean free path in the description of molecular diffusion. This analogy leads to a simple expression for the turbulent viscosity $\nu_{_T}$

$$\nu_{_T} = \ell^2 \left\| \boldsymbol{\nabla} \boldsymbol{v} \right\| \tag{3}$$

For Atmospheric Boundary Layer (ABL), it can be assumed that the horizontal velocity gradients are negligible in comparison to the vertical one. Moreover we suppose that the vertical velocity component tends to zero and also its gradients are negligible. The basic mixing length model (originally proposed by Prandtl) was modified for boundary layer flows by Blackadar (1962) and generalized for stability effects by Estoque and Bhumralkar (1969). For the flow in thermally stratified boundary layer the following stability function $\mathcal{G}$ can be used:

$$\nu_{_T} = \ell^2 \left[\left(\frac{\partial \bar{u}}{\partial z} \right)^2 + \left(\frac{\partial \bar{v}}{\partial z} \right)^2 \right]^{1/2} \mathcal{G} \tag{4}$$

Where the function $\mathcal{G}$ is given by :

$$\begin{aligned} \mathcal{G} &= (1 + \beta\, Ri)^{-2} \qquad \text{for } \; Ri > 0 \\ \mathcal{G} &= (1 - \beta\, Ri)^{2} \qquad \text{for } \; Ri \leq 0 \end{aligned} \tag{5}$$

where β is a constant (≈ 3) and Ri stands for (gradient) Richardson number.

In this way the problem of turbulent closure was reduced to the problem of finding some suitable formula for the mixing length ℓ. The general expression for ℓ, given by von Kármán is:

$$\ell = \frac{-\varkappa\, \partial |\boldsymbol{v}| / \partial z}{\partial^2 |\boldsymbol{v}| / \partial z^2} \tag{6}$$

Here the parameter $\varkappa = 0.36 - 0.41$ is *von Kármán's constant*. The simplest assumption that can be made on ℓ (inside the boundary layer) is that the mixing length is equal zero on the wall and grows linearly with the distance from the surface.

$$\ell = \varkappa\, z \tag{7}$$

This simple linear dependency can give good results in the proximity of wall. At larger distances it is usually replaced by some suitable asymptotic value ℓ_∞. This free-stream mixing length is the tuning parameter that can either be evaluated by experimental fitting or estimated according to some empirical formula.

The above approach was reported e.g. in [1], [5] or [2].

SST $k - \omega$ turbulence model

This two-equation model was chosen as a step up from the elementary algebraic turbulence model that only accounts for local velocity gradients. The aim was to better handle the turbulence history in the flow, including large flow curvature and massive recirculation.

The main idea of this model is an attempt to locally use the better of classical $k - \epsilon$ and $k - \omega$ models, depending the flow regime. The experience shows, that $k - \omega$ model usually performs best close to the wall, while the $k - \epsilon$ model performs better away from the wall. Thus,

following the construction of the original $k-\omega$ model of Wilcox, Menter (1993) created the Shear Stress Transport (SST) $k-\omega$ model using the fact, that both $k-\epsilon$ and $k-\omega$ models can be formulated in the same way (just with different coefficients in the governing equations) and then an automatic blending function can be used to smoothly switch between the two models, depending on local flow conditions. The turbulent viscosity $\mu_{_T} = \rho\nu_{_T}$ can be evaluated from

$$\mu_{_T} = \frac{\rho\, k}{\omega} \tag{8}$$

The turbulent kinetic energy k and specific rate of its dissipation ω can be computed using the following set of transport equations:

$$\frac{\partial \rho k}{\partial t} + \boldsymbol{\nabla}\cdot(\rho k \boldsymbol{v}) = \boldsymbol{\nabla}\cdot\left[\left(\mu + \frac{\mu_{_T}}{\sigma_k}\right)\boldsymbol{\nabla} k\right] + P - \beta^*\rho k\omega \tag{9}$$

$$\frac{\partial \rho \omega}{\partial t} + \boldsymbol{\nabla}\cdot(\rho \omega \boldsymbol{v}) = \boldsymbol{\nabla}\cdot\left[\left(\mu + \frac{\mu_{_T}}{\sigma_\omega}\right)\boldsymbol{\nabla} \omega\right] + \frac{\gamma\rho}{\mu_{_T}}P - \beta\rho\omega^2 + 2\rho\frac{1-F_1}{\sigma_{\omega 2}\omega}\boldsymbol{\nabla} k\cdot\boldsymbol{\nabla}\omega \tag{10}$$

The production of turbulent kinetic energy is computed from the strain rate tensor $\boldsymbol{S} = (\boldsymbol{\nabla}\boldsymbol{v} + \boldsymbol{\nabla}^{_T}\boldsymbol{v})/2$ as

$$P = \mu_{_T} S^2 \quad \text{where} \quad S = \sqrt{2\boldsymbol{S}:\boldsymbol{S}} \tag{11}$$

The coefficients appearing in these equations are described e.g. in [3] or [4].

Numerical solvers

In this paper only the first two codes are discussed and compared:

Finite-Difference Semi-Implicit code

- semi-implicit time discretization
- central in space discretization of second order
- artificial compressibility method for pressure resolution
- non-conservative form of advection terms
- algebraic turbulence closure
- artificial viscosity stabilization

Finite-Volume Explicit code

- explicit time-integration of Runge-Kutta type
- central in space discretization of second order
- artificial compressibility method for pressure resolution
- conservative formulation of advection terms
- SST $k-\omega$ turbulence closure
- non-oscillatory filter stabilization

Computational test case

The computational setup closely follows the experiments that were performed for the same geometry in the environmental windtunnel of the Institute of Thermomechanics of the AS CR. The numerical simulations were performed on a domain of the size of $8100 \times 5850 \times 2700\ m$ (which corresponds to $900 \times 650 \times 300\ mm$ in the model scale). The domain is a part of the region of a real opencast coal mine. This means that the lower boundary of the computational domain is formed by an impermeable, no-slip wall with quite complex terrain profile.

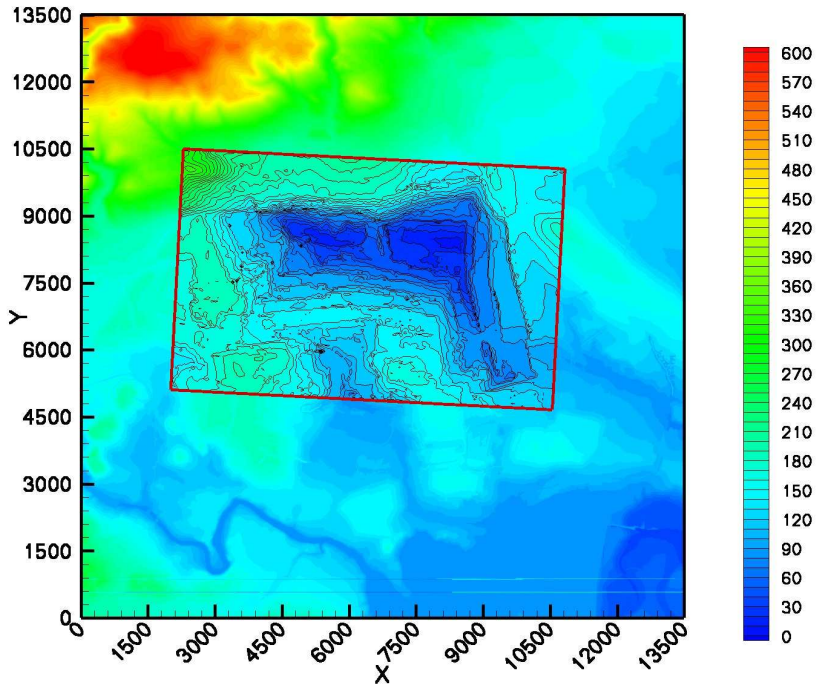

Figure 1: Computational subdomain and its orography profile

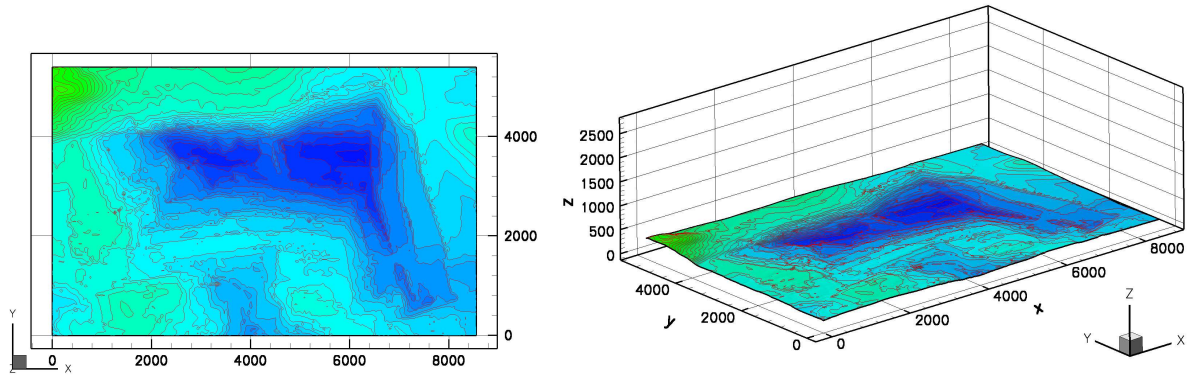

Figure 2: Domain orography profile

The flow is determined by the inflow velocity profile prescribed at $x = 0$. At this boundary the velocity is assumed to be parallel to the x-axis and given by a simple power-law profile, i.e. $u(z) = U_0(z/H_{BL})^{1/7}$. The reference wind velocity $U_0 = 10m \cdot s^{-1}$ and boundary layer thickness is set to $H_{BL} = 1350m$. All other parameters (density, viscosity, ...) correspond to air.

Numerical results

The numerical simulations were performed on a structured, wall fitted grid with $190 \times 120 \times 40$ cells. The grid has horizontally homogeneous resolution (45 meters), while in the vertical direction the grid is refined close to the wall with minimal cell size of $0.2m$. The numerical results presented hereafter were obtained using the semi-implicit finite-difference code[2].

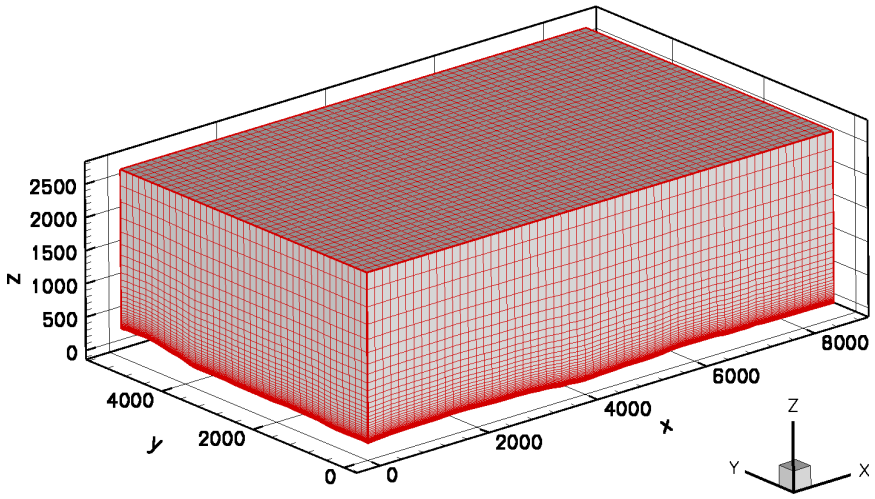

Figure 3: Structure of the computational grid.

The near wall streamlines are shown in the Fig. 4. The deviations of the flow respect the terrain profile that is represented in the figure by the orography elevation contours.

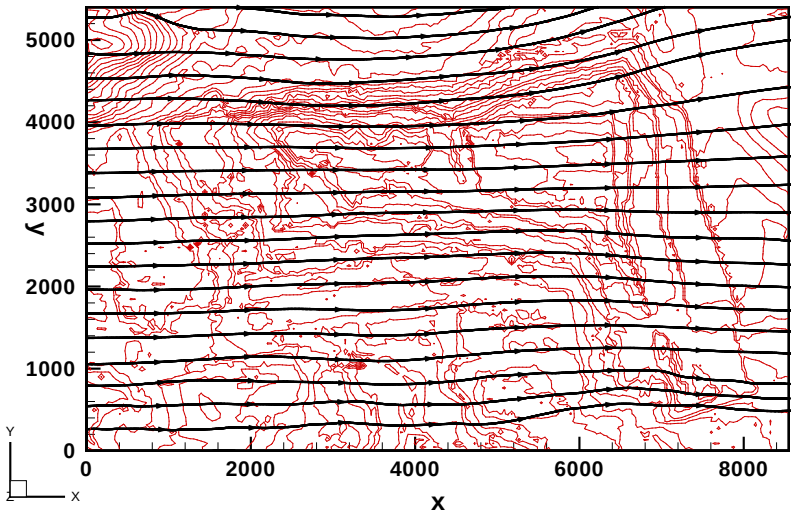

Figure 4: Streamlines in the near-wall layer (approx. $1m$ above terrain).

[2]More results obtained using the other method will be presented during the lecture

Fig. 5 shows the flow acceleration around the edges of orography

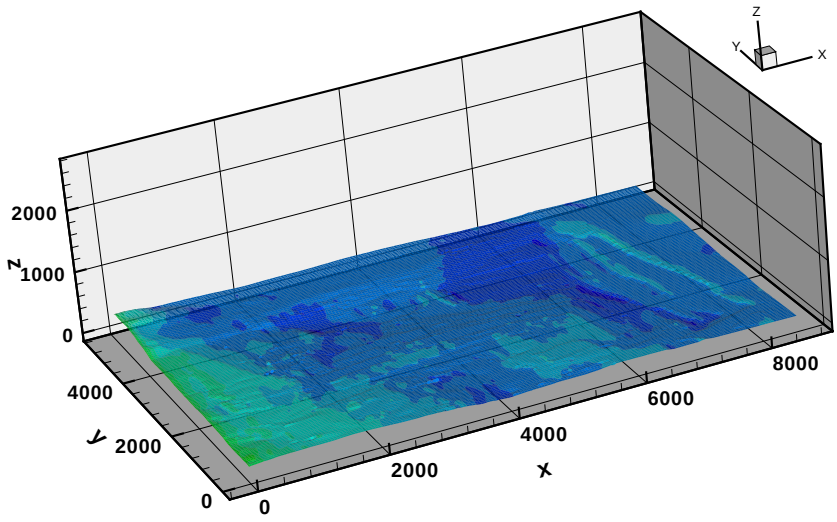

Figure 5: Contours of the dominant u component of the velocity in the near-wall layer (approx. $1m$ above terrain).

Also the regions of ascending/descending flow properly follow the orography as expected.

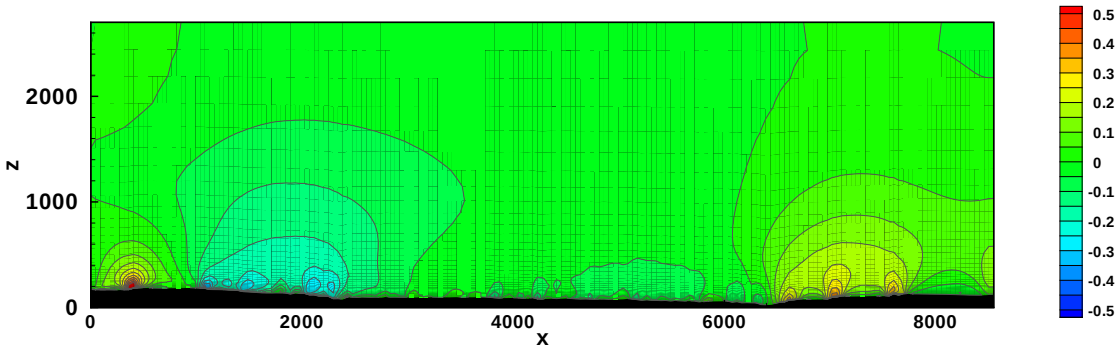

Figure 6: Contours of the vertical velocity component w in a $x - z$ plane of the symmetry of the domain.

Conclusions & Remarks

The first numerical results have demonstrated that both codes produce results that meet our expectations. This means the velocity field as well as the pressure and turbulent viscosity behave as they should from the physical point of view. Also the spatial resolution of the numerical simulations seems to be sufficient to capture the most important topographical features.

The comparison of results obtained using the two above described codes revealed some important facts:

- The flow field predictions from both models are close to each other. This indicates that the mathematical models were successfully implemented into numerical codes. The question is, which of them will produce results closer to reality, i.e. to the experimental results.
- From the point of view of the computational efficiency, the finite-difference code runs significantly faster. This is caused by a simpler numerical scheme being used, but also by the fact that fewer (4 instead of 6) equations are solved due to only algebraic turbulence model. The efficiency of the finite-volume solver has been significantly improved by a specific choice of Runge-Kutta time-stepping scheme and also due to parallelization of the code using OpenMP.
- The finite-volume code seems to be more sensitive to the non-smooth geometry of the no-slip wall. The question, whether this is caused by the turbulence model or by the discretizatiom method, remains to be answered.

The future investigation will focus on detailed comparison of numerical and experimental results for given geometry. Further numerical tests will be performed using other numerical codes in order to estimate the variation of numerical predictions from code to code. This should, together with the comparison with experimental data, provide some elementary information about the reliability of numerical simulations.

Acknowledgment

The financial support for the present project was provided by the grant *TA01020428* of the *Technological Agency of the Czech Republic*.

References

[1] ATKINSON, B. W.: Introduction to the fluid mechanics of meso-scale flow fields. In: *Diffusion and Transport of Pollutants in Atmospheric Mesoscale Flow Fields* (edited by A. GYR & F.-S. RYS), vol. 1 of *ERCOFTAC series*, chap. I., (pp. 1–22). Kluwer Academic Publishers (1995).

[2] BODNÁR, T., BENEŠ, L., & KOZEL, K.: Numerical Simulation of Flow over Barriers in Complex Terrain. *Il Nuovo Cimento C*, vol. 31, no. 5–6: (2008) pp. 619–632.

[3] BODNÁR, T. & PŘÍHODA, J.: Numerical simulation of turbulent free-surface flow in curved channel. *Journal of Flow, Turbulence and Combustion*, vol. 76, no. 4: (2006) pp. 429–442.

[4] HELLSTEN, A.: Some improvements in Menter's $k-\omega$ SST turbulence model. Tech. rep., American Institute of Aeronautics and Astronautics (1998). AIAA-98-2554.

[5] MASON, P. J. & KING, J. C.: Measurements and predictions of flow and turbulence over an isolated hill of moderate slope. *Quarterly Journal of the Royal Meteorological Society*, vol. 111: (1985) pp. 617–640.

[6] PRANDTL, L.: The Mechanics of Viscous Fluids. In: *Aerodynamic Theory* (edited by W. F. DURAND), vol. III., chap. G., (pp. 35–208). Julius Springer (1935).